

# Engineered swift equilibration of a Brownian particle

3 Ignacio A. Martínez<sup>1</sup>, Artyom Petrosyan<sup>1</sup>, David Guéry-Odelin<sup>2</sup>,  
Emmanuel Trizac<sup>3</sup>, Sergio Ciliberto<sup>1</sup>

1 : Laboratoire de Physique, CNRS UMR5672  
Université de Lyon, École Normale Supérieure,  
46 Allée d'Italie, 69364 Lyon, France.

2 : Laboratoire Collisions Agrégats Réactivité, CNRS UMR5589,  
Université de Toulouse, 31062 Toulouse, France

3 : LPTMS, CNRS, Univ. Paris-Sud, Université Paris-Saclay,  
91405 Orsay, France

4 April 1, 2016

## 5 1 Generalized ESE protocol

6 When the system is manipulated by a non harmonic potential  $U(x, t)$ , the position distribution  
7 is no longer Gaussian, either in equilibrium or out of equilibrium. In this case, one has to solve  
8 the following Fokker-Planck equation for the over damped situation considered here

$$\partial_t \rho(x, t) = \frac{1}{\gamma} \partial_x [\rho \partial_x (U)] + D \partial_{xx}^2 \rho. \quad (1)$$

9 This relation is linear in  $U$ , so that when the target distribution  $\rho(x, t)$  has been chosen, it is  
10 possible to express the associated external potential  $U$  that will guarantee the desired dynamics,  
11 as

$$U(x, t) = -k_B T \log \rho(x, t) + k_B T \int^x dy \left\{ \frac{\int^y \partial_t \rho(z, t) dz}{\rho(y, t) D} \right\}. \quad (2)$$

12 As an illustration, considering  $\rho$  of Gaussian form, we recover all the results derived in the  
13 main text, and in particular the dynamical equation connecting  $\alpha$  and  $\kappa$ . Beyond the harmonic  
14 case, taking  $\rho(x, t)$  of the form  $\exp(-\beta x^4)$  (up to normalization), we can compute explicitly  
15 the confining potential  $U/(k_B T) = \beta x^4 + Ax^2$ . Once the evolution law  $\beta(t)$  is chosen, the  
16 only unknown  $A$  follows from  $A = (4D)^{-1} d \log \beta / dt$ . Hence, the decompression of a state in

17  $\exp(-\beta x^4)$ , which requires that  $\dot{\beta}$  be negative in some time window, yields a negative value of  $A$ ,  
18 which corresponds to a drive with a bistable potential  $U$ . The argument readily extends to target  
19 densities of the form  $\rho(x, t) \propto \exp(-\beta x^n)$  where we find a driving potential  $U/(k_B T) = \beta x^n + Ax^2$   
20 with  $A = (nD)^{-1} d \log \beta / dt$ .

## 21 **2 Data analysis**

### 22 **2.1 System dynamics**

23 Figure S1 shows a set of trajectories for both processes, ESE and STEP. This highlights the  
24 impossibility to define equilibrium following solely a single trajectory. Equilibrium is indeed a  
25 statistical notion.

26 The linearity of Langevin equation in the case of a harmonic potential guarantees the Gaus-  
27 sianity of the position probability density function  $\rho(x, t)$ . Experimentally, the Gaussianity of a  
28 data set is quantified through its kurtosis. This parameter is defined from the centered fourth  
29 moment  $\mu_x$  and the standard deviation  $\sigma_x$  of the distribution:  $\text{Kurt}(x) = \mu_x / \sigma_x^4$ . For a Gaus-  
30 sian distribution, we have  $\text{Kurt}(x) = 3$ . The experimental values of the kurtosis along the ESE  
31 protocol are displayed in Fig. S2, illustrating how the distribution remains Gaussian during the  
32 whole process.

### 33 **2.2 Experimental uncertainties.**

34 The system is calibrated with standard techniques such as equipartition theorem and power  
35 spectral density [1]. The calibration factor of the photodiode is  $S = (2666 \pm 3) \text{nm/V}$ . The  
36 absolute errors of the system's observables are  $\Delta\kappa = 0.03 \text{pN}/\mu\text{m}$  and  $\Delta x = 0.1 \text{nm}$ . Then, to  
37 obtain the total error of the measures, the statistical uncertainty is calculated with a confidence  
38 interval of 99 % over the  $N = 2 \cdot 10^4$  cycles. This yields an error of about 1% on the standard  
39 deviation of the position. Finally, in the case of the cumulative energetics of both processes,  
40 fluctuations are intrinsic as the system is in contact with a thermal bath. Thermal fluctuations  
41 produce a constant exchange of energy between the system and its environment, as heat, even  
42 with no change in the control parameter. The variance of heat is consequently larger than the  
43 variance of the work.

### 44 **2.3 Range of validity of the method**

45 How fast can we run the ESE protocol? In our particular experimental case, the shortest time  
46 is set by the validity of the model, together with experimental limitations. We start with  
47 the first point. Our description is overdamped, and neglects the inertial term in the Langevin  
48 equation. This is admissible provided we do not tamper the rapid ballistic regime, which requires

49  $t_f > m/\gamma \simeq 1\mu\text{s}$ , where  $m$  is the colloid mass and  $\gamma$  is the viscosity term [2]. For shorter times,  
50 the underdamped extension of the problem must be taken into account.

51 We next address the experimental limitations of our setup. We chose the process time as 0.5  
52 ms as a compromise between the relaxation time, the maximum acquisition frequency  $f_{\text{acq}} = 20$   
53 kHz and the maximum stiffness we can achieve,  $\kappa_{\text{max}} \simeq 50\text{pN}/\mu\text{m}$ . The time evolution of the  
54 trap stiffness is indeed non-monotonous, reaching an extremum that significantly exceeds the  
55 final value. The experimental stiffness being proportional to the optical power available, a more  
56 powerful laser will allow for a decrease of the ESE time  $t_f$ .

## 57 References

- 58 [1] K. Svoboda and S. M. Block, “Biological applications of optical forces,” *Annual review of*  
59 *biophysics and biomolecular structure*, vol. 23, no. 1, pp. 247–285, 1994.
- 60 [2] T. Li, S. Kheifets, D. Medellin, and M. G. Raizen, “Measurement of the instantaneous  
61 velocity of a brownian particle,” *Science*, vol. 328, no. 5986, pp. 1673–1675, 2010.

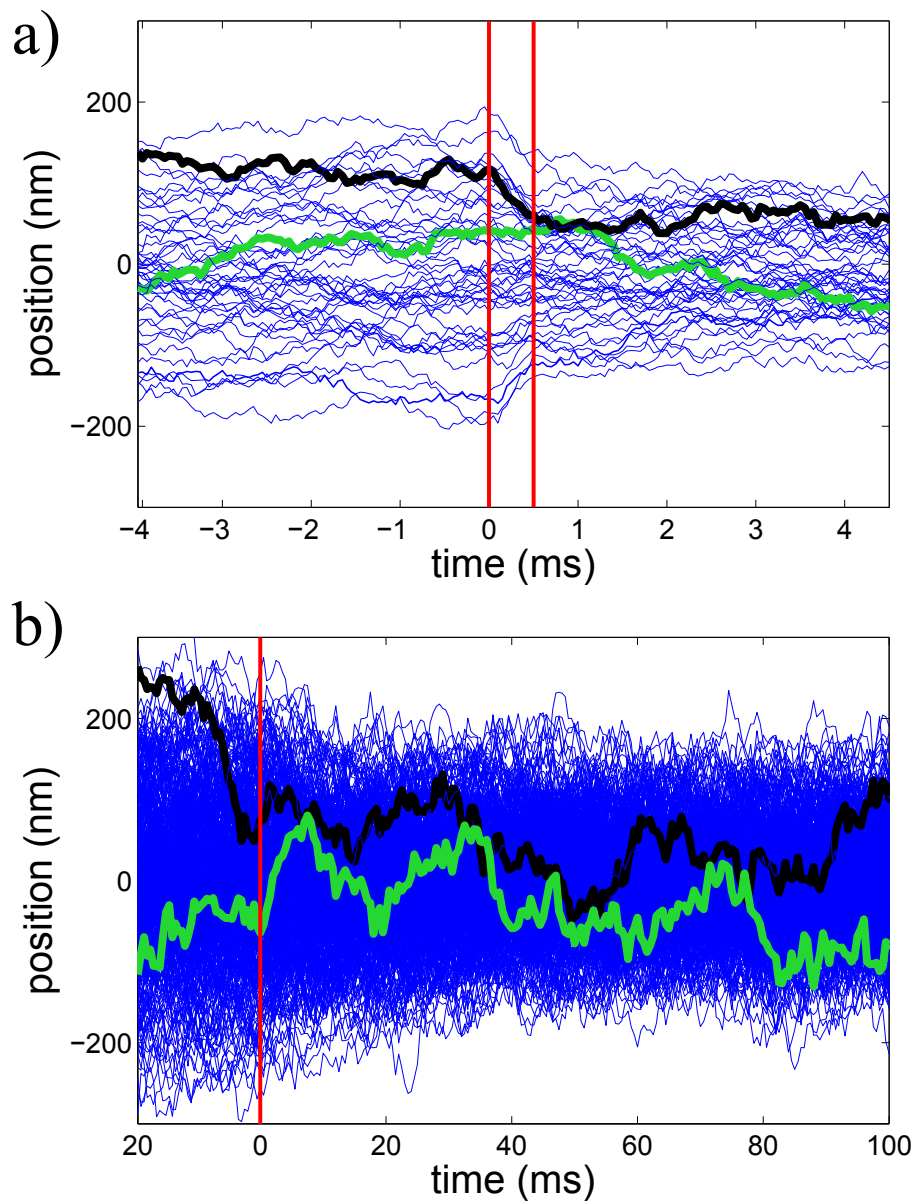


Figure S1: **Different sets of trajectories for the two different processes.** a) ESE protocol. b) STEP protocol. In each case, we highlight two particular trajectories (thick green and black lines) to show the difficulty of observing equilibration at such a level of description. In a), vertical red lines represent the initial and final times of the protocol. In b), the vertical red line represents the time instant when the potential landscape is abruptly changed.

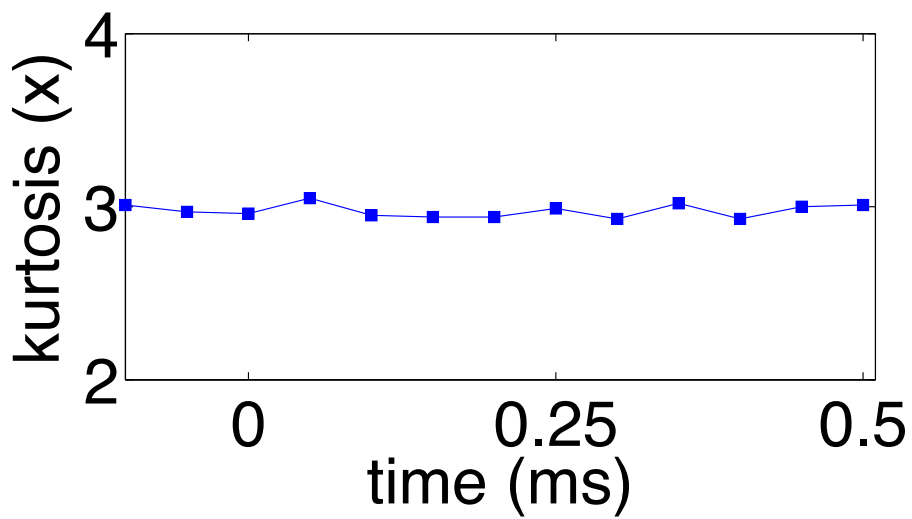


Figure S2: Experimental measure of the position distribution kurtosis  $Kurt(x)$  during the ESE protocol. Statistical errors are below the symbol size.